Hindawi Publishing Corporation
Journal of Chemistry
Volume 2016, Article ID 3508307, 6 pages
http://dx.doi.org/10.1155/2016/3508307

Research Article

AC Humidity Sensing Properties of Mesoporous K_2CO_3-SiO_2 Composite Materials

Liang Guo,[1,2] Xuefeng Chu,[1,2] Xiaohong Gao,[1,3] Chao Wang,[1,3] Yaodan Chi,[1,3] and Xiaotian Yang[1,3]

[1]*Jilin Provincial Key Laboratory of Architectural Electricity & Comprehensive Energy Saving, Jilin Jianzhu University, Changchun 130118, China*
[2]*Department of Basic Science, Jilin Jianzhu University, Changchun 130118, China*
[3]*School of Electrical Engineering and Computer, Jilin Jianzhu University, Changchun 130118, China*

Correspondence should be addressed to Xiaotian Yang; hanyxt@163.com

Received 14 February 2016; Accepted 21 March 2016

Academic Editor: Yves Grohens

The mesoporous silica SBA-15 and mesoporous K_2CO_3-SiO_2 composite material were synthesized. Characterization of microstructure and morphology of materials indicated that the composite material had saved the porous framework of mesoporous silica SBA-15. Humidity sensing properties of different inverse proportion K_2CO_3-SiO_2 composite material were studied and we found that the sample with 0.16 g/g K_2CO_3 exhibited excellent linearity in the wide humidity range. The complex impedance changed five orders of magnitude from 11% RH to 95% RH. The rapid response and recovery time were 10 s and 38 s, respectively. Finally a feasible ion transfer mechanism was brought forward to explain the sensing mechanism.

1. Introduction

Humidity sensor is a class of widely used chemical sensor. For the raring demand of the industrial processing and the environmental control, more and more researchers are interested in humidity sensor. The growing demands of controlling water vapor led to considerable interests in the development of sensing materials. In recent years, materials that have been studied for this purpose mainly include organic polymers [1–4], metal oxide ceramics [5–10], and porous materials [11–15]. Among the porous materials mesoporous silica SBA-15 exhibits good properties such as environment stability, wide range of work temperature, and quick response-recovery properties [13, 14]. Therefore, mesoporous silica SBA-15 becomes a promising candidate for humidity and gas sensing material [13–15]. However, the pure mesoporous silica SBA-15 exhibits its humidity sensitivity only over 75% RH. In order to improve its humidity sensitivity, adulteration was a widely used method. There were many reports about the addition of alkali metal ions to improve the humidity sensitivity [16–18]. Some papers were about K^+ which exhibits favorable effect in improving humidity sensitivity [16, 17].

In 2009 Yuan et al. have successfully doped K^+ into SBA-15 and greatly improved its humidity sensing properties [19]. In that work, K^+ was doped into SBA-15 material by thermal dispersion. Though the humidity sensing properties were greatly improved after thermal dispersion, the mesoporous structure was seriously destroyed. In this work, we doped K^+ into SBA-15 material by solution dispersion. The characterized results indicated that this simple method can successfully adulterate K^+ into SBA-15 material and the mesoporous structure was fully saved. Humidity sensing properties were tested and the results indicated that less doped amount could reveal the same effect (the 0.16 g/g K^+-doped sample exhibits the best humidity sensitivity; in the prevenient study it was the 0.8 g/g K^+-doped sample [19]). Moreover, the response and recovery times are quicker than before. At last, an ion transfer sensing mechanism of appropriate K^+-doped SBA-15 humidity sensor was discussed.

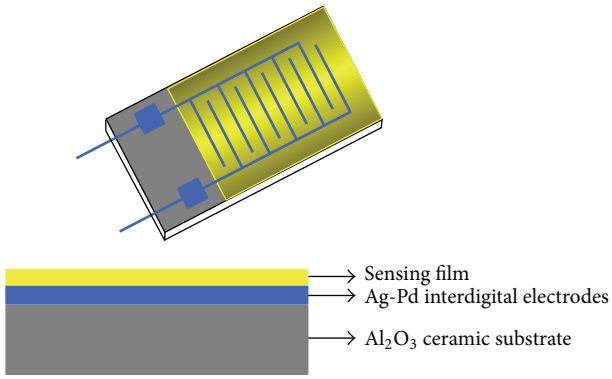

Figure 1: The electrode configuration structure of the humidity sensor.

2. Experimental

2.1. Preparation of Sensing Materials. The mesoporous silica SBA-15 was synthesized with the method reported by Li and Zhao [20]. In a typical synthesis, 2.0 g of poly(ethylene glycol)-block-poly(propylene glycol)-block-poly(ethylene glycol) ($EO_{20}PO_{70}EO_{20}$, P123, averaged molecular weight = 5800, Aldrich) was dissolved in a mixture of 15 mL deionized water and 60 mL 2 M HCl under stirring. Then 4.4 g of tetraethyl orthosilicate (TEOS, 98%, Aldrich) was added dropwise to the solution at 40°C. The resultant mixture was stirred continuously for 24 hours, and then it was aged at 60°C for 24 hours without stirring. The precipitate was in turn filtered, washed with deionized water, and dried at 100°C overnight. The obtained powders were heated to 550°C at a ramp rate of 1°C/min and calcined at this temperature in air for 8 hours to remove the surfactant.

The K_2CO_3-SiO_2 composite materials were prepared by solution adulterate method. The SBA-15 was impregnated with K_2CO_3 aqueous solution of a desired amount. The resulting material was then dried at 100°C in air overnight and then ground homogeneously. In our work, the different inverse proportion of K_2CO_3 was 0.08 g, 0.16 g, 0.8 g, and 1.44 g in 1 g SBA-15, respectively.

2.2. Methods of Characterization. The powder XRD patterns were measured by a D8 Tools X-ray diffraction instrument using the Cu Kα radiation at 40 kV and 30 mA. Infrared spectra were taken on a Perkin-Elmer series with a resolution of 4 cm^{-1}. The samples were prepared in a form of KBr pellet, of which the thickness is about 1.3 mm. Each spectrum was collected at room temperature under atmospheric pressure. Field emission scanning electron microscopy (SEM) images were obtained using a JEOL JSM-7500F microscope. N_2 adsorption-desorption isotherms were measured at 77 K on a Micromeritics ASAP 2010 m instrument (Micromeritics Instrument Corp., Norcross, GA). The sensing material was spin-coated on the interdigital electrodes (6 mm × 3 mm × 1 mm) made of Al_2O_3; the electrode configuration structure of the impedance-type humidity sensor was showed in Figure 1. The humidity sensitivity was done by a ZL-5 intelligent LCR analyzer (made in Shanghai, China) at room temperature. The resolution of the analyzer is 0.01%. The frequency range of the analyzer is 12 Hz–100 kHz. The impedance of the analyzer is 0.00001 Ω–99999 kΩ. The controlled humidity environments were obtained with saturated salt solutions in a closed glass vessel.

3. Results and Discussion

3.1. X-Ray Diffraction. The low angle XRD spectrum was given in Figure 2(a). We could see the peak attributed to (100) of SBA-15 was obtained in all the doped samples, indicating that the ordered mesoporous structure of SBA-15 was not destroyed after introducing K_2CO_3 into SBA-15. It was obvious to notice that, with the increasing of K_2CO_3 content, the (100) peak of different K_2CO_3-SiO_2 composite material shifted to the higher angle direction, which suggests that the introduction of K_2CO_3 resulted in the shrinkage of the pore wall of SBA-15.

As Figure 2(b) showed, we can see that all the samples have a broad peak centered at $2\theta = 21.7°$, demonstrating that the pore wall of all the samples was amorphous, with the level of K_2CO_3 content increasing, and the peaks of K_2CO_3 appeared and become stronger.

3.2. IR Spectroscopy. Figure 3 displayed infrared spectra of all the products. As we can see, for pure SBA-15, the characteristic peaks at 1635 and 950 cm^{-1} were attributed to Si–OH, and the peaks of Si–O–Si were observed at 1092 and 808 cm^{-1}. All the bands were similar to the results of literature [14, 21]. It was interesting to note that the peak of 1635 cm^{-1} was very weak for pure SBA-15 compared to other samples. Because of the hydrophilic property of K_2CO_3, the more water molecules were adsorbed as the level of K_2CO_3 increased. Then, the water molecules interacted with the Si–O–Si of SBA-15 to form the surface hydroxyls. When the content of K_2CO_3 increased beyond 0.16 g/g, it would adsorb more water molecules, and H^+ was released by some of the hydroxyls, so that the hydroxyls on the surface would decrease. In addition, specific peaks of C–O asymmetric stretching vibrational modes and the in-plane deformation mode appeared at 1395 cm^{-1} and 703 cm^{-1} and gradually became stronger with the increasing K_2CO_3 level. This was in agreement with the result of wide angle XRD.

3.3. SEM Characterization. The morphology of SBA-15 and a representative image of K_2CO_3-SiO_2 composite material were shown in Figure 4. It can be seen from Figure 4(a) that mesoporous SBA-15 consisted of some short rods. Figure 4(b) showed that no evident difference was observed after adding of K_2CO_3. This phenomenon indicated that the mesoporous structure of SBA-15 was fully saved after adding of K_2CO_3.

3.4. N_2 Adsorption-Desorption Characterization. To character the nature of our samples farther, we chose pure SBA-15 and K_2CO_3 content of 0.16 g/g K_2CO_3-SiO_2 composite material to test N_2 adsorption-desorption. The curve was shown in Figure 5. From the figure, we can see that the trace

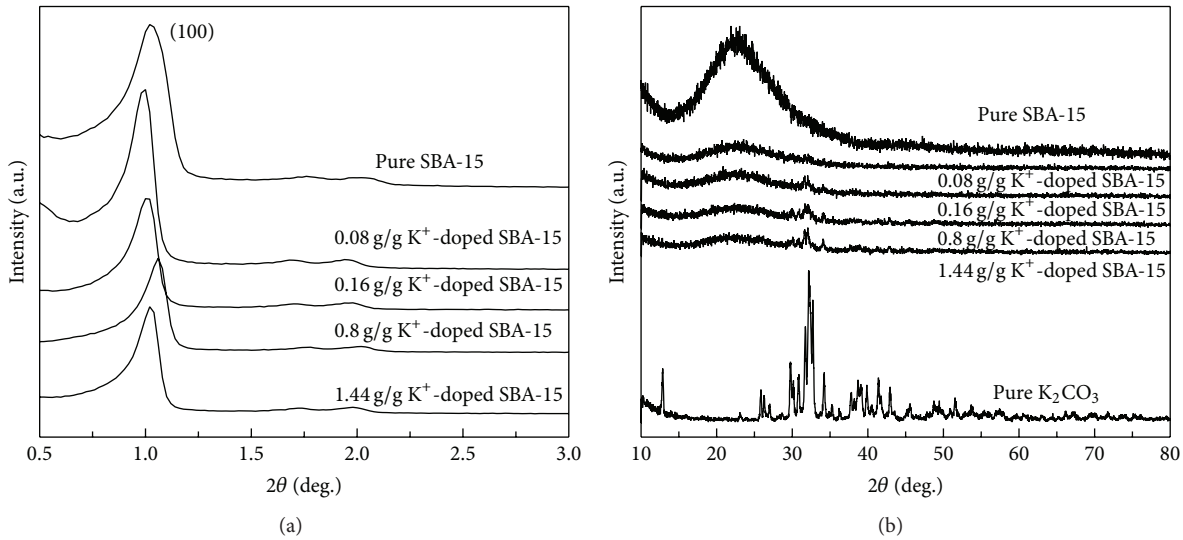

Figure 2: Lower angle (a) and wide angle (b) XRD spectra of the materials.

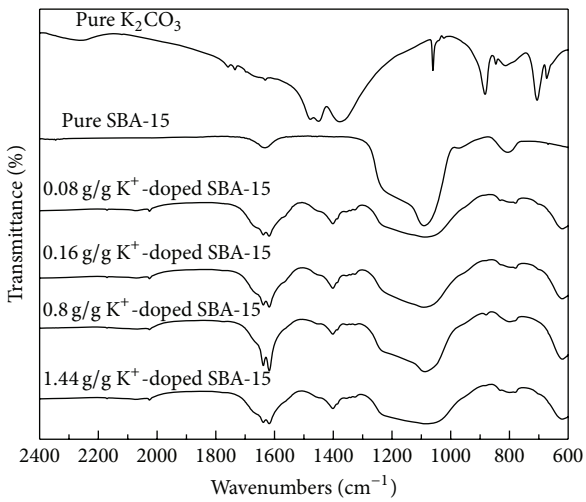

Figure 3: IR spectra of the materials.

of SBA-15 was type IV; after the addition of K_2CO_3 as obtained in Figure 5(a) the shape of type IV was still retained, illuminating that fact that the mesoporous structure was reserved in the sample of K_2CO_3-SiO_2 composite material (K_2CO_3 content of 0.16 g/g). Otherwise, the step inflexion (p/p_0) of K_2CO_3-SiO_2 composite material (K_2CO_3 content of 0.16 g/g) was smaller than that of pure SBA-15, suggesting the corresponding pore size shrink with the added K_2CO_3. This was consonant with the result of the pore size distribution curves as shown on Figure 5(b). From Figure 5(b) we can see the BJH pore diameter was changed from 6.25 nm of pure SBA-15 to 5.99 nm of K_2CO_3-SiO_2 composite material (K_2CO_3 content of 0.16 g/g) and the BET surface area shifted from 592 m^2/g of pure SBA-15 to 385 m^2/g of K_2CO_3-SiO_2 composite material (K_2CO_3 content of 0.16 g/g). All the results were in agreement with XRD, IR, and SEM above.

3.5. Humidity Sensing Properties of SBA-15 Doped with K_2CO_3

3.5.1. RH-Impedance Curves. Figure 6 showed the dependence of impedance with relative humidity (RH) for pure SBA-15 and K_2CO_3-SiO_2 composite material. The test frequency was 100 Hz and the applied voltage was 1 V. It could be seen obviously from the figure that the pure SBA-15 does not reveal humidity sensing properties until the relative humidity reaches 75% RH, while the K_2CO_3-SiO_2 composite material could reveal humidity sensing properties in the whole RH range. With the K_2CO_3 content increasing, the impedance decreased sharply at low RH but did not evidently at high RH. An appropriate adulterate method could improve the humidity sensing properties of pure SBA-15; on the contrary superfluous adulterate method could influence the materials humidity sensing property. The result indicated that the K_2CO_3 content of 0.16 g/g K_2CO_3-SiO_2 composite material had the best linearity; thus all the discussions below concerned this sample.

3.5.2. Response and Recovery Characteristic. In order to check the practicability of the sensor, the response and recovery characteristic were given in Figure 7. According to literature [22], the response and recovery time were defined as the time taken to reach 90% of the total impedance change. For this sample the response time was about 10 s by increasing from 11% RH to 95% RH, and the recovery time was about 38 s by decreasing from 95% RH to 11% RH. The results showed that this sensor achieved the practice application standard.

3.5.3. Complex Impedance Property. Figure 8 gives the complex impedance plot of this sensor at different RH range. We magnified the real part and imaginary part on the same plane to compare the complex impedance plots more conveniently. The test frequency was from 20 Hz to 100 kHz, and the RH range from 11% RH to 95% RH at room temperature. It can

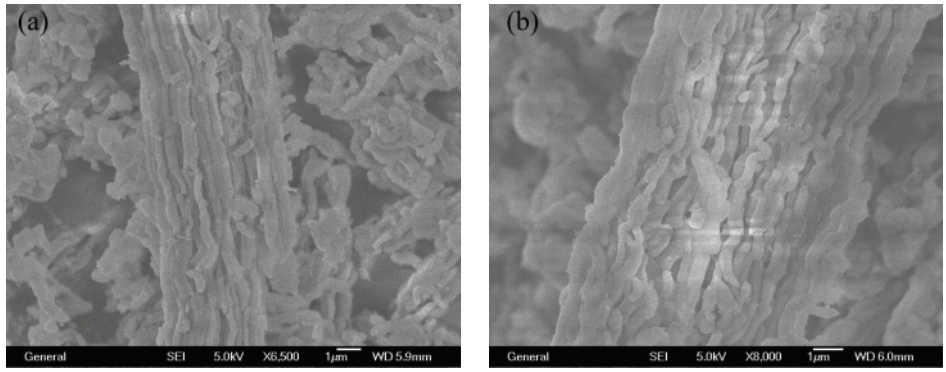

(a) (b)

Figure 4: SEM image of (a) SBA-15 and (b) K_2CO_3-doped SBA-15.

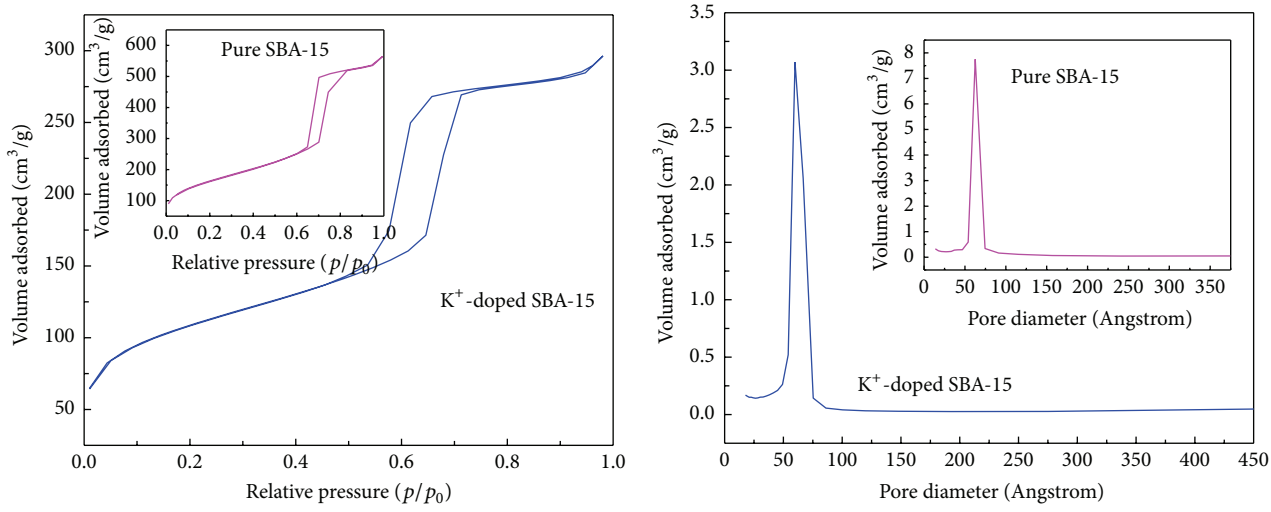

(a) (b)

Figure 5: (a) Nitrogen adsorption-desorption isotherms. (b) Pore size distribution of pure and K^+-doped SBA-15.

be seen clearly from the plots that at very low RH range only a half of a semicircle was observed. With increasing the RH, the region of the semicircle increased to become a complete semicircle. However the RH value reached over 54% RH, the semicircle became disappeared, and a little straight line turned out in our test frequency range. The appearance of a new curve representative of another electric particle became contributing to conductance. The higher the RH value was, the more patent the straight line was. When the RH value reached 95% RH the semicircle disappeared absolutely in this test frequency range and left a straight line only.

3.6. Mechanism of Humidity Sensing Properties. In this part, we try to give a feasible mechanism of this humidity sensor based on the above results. For pure SBA-15 owing to its high impedance nature, it showed a poor humidity sensitive property until RH range reached 75% RH. However, the humidity sensing properties improved obviously after K^+-doped. The complex impedance changed five orders of magnitude from 11% to 95% RH. At very low RH range water molecule was so little that the coverage of water on the surface was not continuous. Thereby protons moved by hopping transmission across the surface [23] and simultaneity proton bonding to water molecule and formed hydronium ions ($H_2O + H^+ = H_3O^+$). At the same time the transfer of H^+ and H_3O^+ was difficult on this discontinuous water layer, so that the impedance was relatively high at low RH range. When the water molecule increased and RH reached middle region the surface coverage was complete and several serial water layers were formed. Here according to the ion transfer mechanism of Grotthuss, $H_2O + H_3O^+ \rightarrow H_3O^+ + H_2O$ [24], H^+ and H_3O^+ transfer were dominating. With increase in the RH, some K^+ came from the ionization of K_2CO_3 based on $K_2CO_3 + H_2O \rightarrow KOH + KHCO_3$. And ions also participated in the conduction. Corresponding to the complex impedance plot this case was semicircle and straight line appeared simultaneously. When the RH reaches the high region, the more K_2CO_3 ionize based on $K_2CO_3 + 2H_2O \rightarrow 2KOH + H_2CO_3$, and then the K^+ ions dominate in the conduction. As we all know, the ionization ability of KOH is much stronger

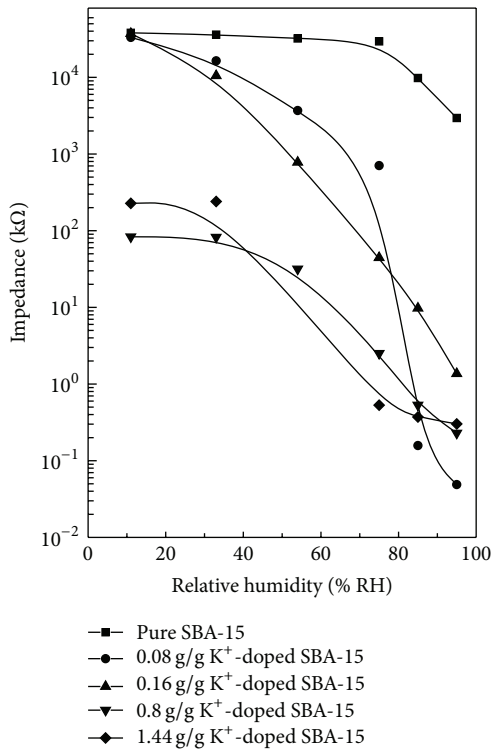

Figure 6: The dependence of resistance on RH for pure SBA-15 and K^+-doped samples.

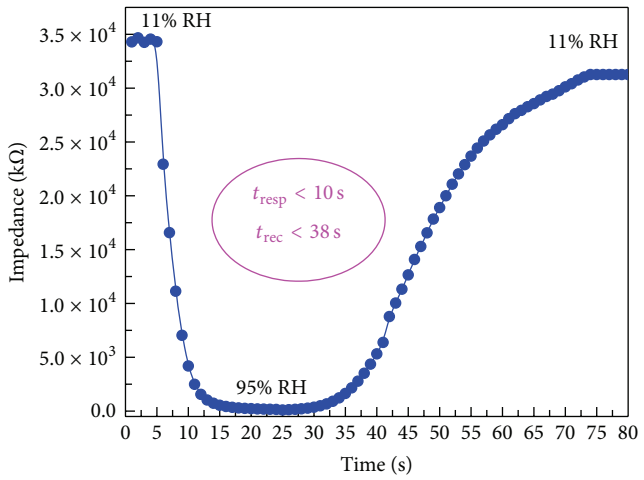

Figure 7: The response and recovery properties of humidity sensor.

than that of $KHCO_3$, so that in this stage the amount of K^+ ions was quite greater than that of the middle region. Corresponding to the complex impedance plot, the curve was only a straight line left. The quick transfer of ions on the water layer results in a sharp decrease of the impedance. Therefore compared to the initial impedance, the value continuously decreases by more than five orders of magnitude.

4. Conclusion

In this work, the pure SBA-15 and K_2CO_3-SiO_2 composite material film of impedance-type humidity sensors were fabricated. The microstructure and morphology of materials were characterized by X-ray powder diffraction (XRD), IR spectroscopy, SEM, and N_2 adsorption-desorption. Their humidity sensing properties were studied and we found that the K_2CO_3 content of 0.16 g/g K_2CO_3-SiO_2 composite material exhibited excellent linearity in the wide humidity range. The rapid response and recovery time were obtained. The mechanism of humidity sensing properties was also discussed.

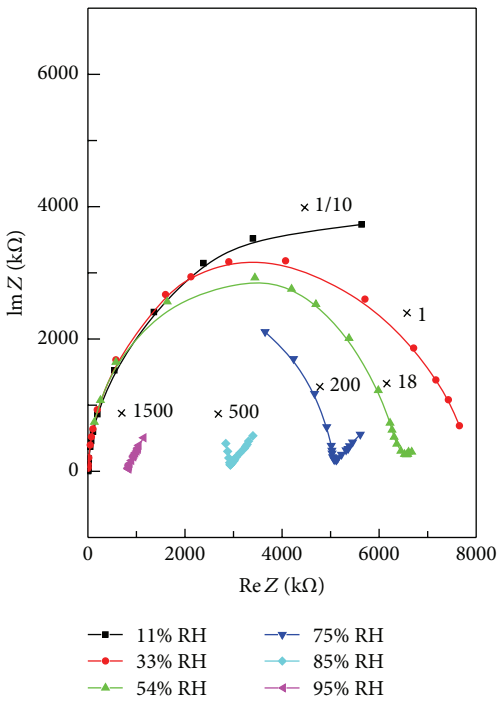

Figure 8: Complex impedance plots in wide humidity environments.

Disclosure

This paper been written by the stated authors who are all aware of its content and approve its submission.

Competing Interests

No competing interests exist in the submission of this paper.

Authors' Contributions

Liang Guo, Xuefeng Chu, Xiaohong Gao, Chao Wang, Yaodan Chi, and Xiaotian Yang have read and approve this version of the paper, and due care has been taken to ensure the integrity of the work.

Acknowledgments

The authors gratefully acknowledge the support from the Natural Science Foundation of Jilin Province (no. 20140520120JH and no. 20140520080JH) and National Natural Science Foundation of China (no. 51272089).

References

[1] M. Y. Lim, H. Shin, D. M. Shin, S. S. Lee, and J. C. Lee, "Poly(vinyl alcohol) nanocomposites containing reduced graphene oxide coated with tannic acid for humidity sensor," *Polymer*, vol. 84, pp. 89–98, 2016.

[2] M. V. Fuke, A. Vijayan, M. Kulkarni, R. Hawaldar, and R. C. Aiyer, "Evaluation of Co-polyaniline nanocomposite thin films as humidity sensor," *Talanta*, vol. 76, no. 5, pp. 1035–1040, 2008.

[3] R. Kumar and B. C. Yadav, "Humidity sensing investigation on nanostructured polyaniline synthesized via chemical polymerization method," *Materials Letters*, vol. 167, pp. 300–302, 2016.

[4] M.-I. Georgaki, A. Botsialas, P. Argitis et al., "1-D polymeric photonic crystals as spectroscopic zero-power humidity sensors," *Microelectronic Engineering*, vol. 115, pp. 55–60, 2014.

[5] S. M. Ke, H. T. Huang, H. Q. Fan, H. L. W. Chan, and L. M. Zhou, "Structural and electric properties of barium strontium titanate based ceramic composite as a humidity sensor," *Solid State Ionics*, vol. 179, no. 27—32, pp. 1632–1635, 2008.

[6] S. A. Makhloufa and K. M. S. Khalil, "Humidity sensing properties of NiO/Al_2O_3 nanocomposite materials," *Solid State Ionics*, vol. 164, no. 1-2, pp. 97–106, 2003.

[7] H. Aoki, Y. Azuma, T. Asaka, M. Higuchi, K. Asaga, and K. Katayama, "Improvement of response characteristics of TiO_2 humidity sensors by simultaneous addition of Li_2O and V_2O_5," *Ceramics International*, vol. 34, no. 4, pp. 819–822, 2008.

[8] I. C. Cosentino, E. N. S. Muccillo, and R. Muccillo, "The influence of Fe_2O_3 in the humidity sensor performance of ZrO_2:TiO_2-based porous ceramics," *Materials Chemistry and Physics*, vol. 103, no. 2-3, pp. 407–414, 2007.

[9] V. K. Tomer, S. Duhan, A. K. Sharma, R. Malik, S. P. Nehra, and S. Devi, "One pot synthesis of mesoporous ZnO–SiO_2 nanocomposite as high performance humidity sensor," *Colloids and Surfaces A: Physicochemical and Engineering Aspects*, vol. 483, pp. 121–128, 2015.

[10] S. Upadhyay and P. Kavitha, "Lanthanum doped barium stannate for humidity sensor," *Materials Letters*, vol. 61, no. 8-9, pp. 1912–1915, 2007.

[11] V. K. Tomer, S. Devi, R. Malik, S. P. Nehra, and S. Duhan, "Fast response with high performance humidity sensing of Ag–SnO_2/SBA-15 nanohybrid sensors," *Microporous and Mesoporous Materials*, vol. 219, pp. 240–248, 2016.

[12] P. Kapa, L. Pan, A. Bandhanadham et al., "Moisture measurement using porous aluminum oxide coated microcantilevers," *Sensors and Actuators B: Chemical*, vol. 134, no. 2, pp. 390–395, 2008.

[13] L. B. Kong, L. Y. Zhang, and X. Yao, "Preparation and properties of a humidity sensor based on LiCl-doped porous silica," *Journal of Materials Science Letters*, vol. 16, no. 10, pp. 824–826, 1997.

[14] C.-T. Wang and C.-L. Wu, "Electrical sensing properties of silica aerogel thin films to humidity," *Thin Solid Films*, vol. 496, no. 2, pp. 658–664, 2006.

[15] J. Yang, K. Hidajat, and S. Kawi, "Synthesis of nano-SnO_2/SBA-15 composite as a highly sensitive semiconductor oxide gas sensor," *Materials Letters*, vol. 62, no. 8-9, pp. 1441–1443, 2008.

[16] Z. Wang, C. Chen, T. Zhang et al., "Humidity sensitive properties of K^+-doped nanocrystalline $LaCo_{0.3}Fe_{0.7}O_3$," *Sensors and Actuators, B: Chemical*, vol. 126, no. 2, pp. 678–683, 2007.

[17] P. G. Su and C. S. Wang, "In situ synthesized composite thin films of MWCNTs/PMMA doped with KOH as a resistive humidity sensor," *Sensors and Actuators B: Chemical*, vol. 124, no. 2, pp. 303–308, 2007.

[18] D. Wang, Y. L. Lou, R. Wang et al., "Humidity sensor based on Ga_2O_3 nanorods doped with Na^+ and K^+ from GaN powder," *Ceramics International*, vol. 41, no. 10, pp. 14790–14797, 2015.

[19] Q. Yuan, W. Geng, N. Li et al., "Study on humidity sensitive property of K2CO3-SBA-15 composites," *Applied Surface Science*, vol. 256, no. 1, pp. 280–283, 2009.

[20] G. Li and X. S. Zhao, "Characterization and photocatalytic properties of titanium-containing mesoporous SBA-15," *Industrial & Engineering Chemistry Research*, vol. 45, no. 10, pp. 3569–3573, 2006.

[21] P.-G. Su, Y.-L. Sun, C.-S. Wang, and C.-C. Lin, "Humidity sensing and electrical properties of hybrid films prepared from [3-(methacrylamino)propyl] trimethyl ammonium chloride, aqueous monodispersed colloidal silica and methyl methacrylate," *Sensors and Actuators B: Chemical*, vol. 119, no. 2, pp. 483–489, 2006.

[22] J.-H. Cho, J.-B. Yu, J.-S. Kim, S.-O. Sohn, D.-D. Lee, and J.-S. Huh, "Sensing behaviors of polypyrrole sensor under humidity condition," *Sensors and Actuators, B: Chemical*, vol. 108, no. 1-2, pp. 389–392, 2005.

[23] J. H. Anderson and G. A. Parks, "The electrical conductivity of silica gel in the presence of adsorbed water," *Journal of Physical Chemistry*, vol. 72, no. 10, pp. 3662–3668, 1968.

[24] F. M. Ernsberger, "The nonconformist ion," *Journal of the American Ceramic Society*, vol. 66, no. 11, pp. 747–750, 1983.